CHAPTER IV
RESULTS AND DISCUSSION

4.1 Catalyst Characterization

This research studied the biodiesel production in a fixed-bed reactor using two different types of heterogeneous basic catalyst. Our previous work, Iangthanarat (2008), firstly used KOH/ZrO_2 and KOH/mordenite as a solid base catalyst via the transesterification reaction in a batch reactor. In order to investigate the optimum conditions for this reaction, two types of catalysts were varied with many parameters, such as the amount of K loading and calcination temperature. It was concluded that the optimum condition for catalysts were 20 wt% loading amount of K calcined at 500°C and uncalcined for KOH/ZrO_2 and KOH/mordenite, respectively. In this work, the optimum condition for catalysts was used with different type of reactor. In order to ensure the efficiency of catalysts, further characterization of the optimum condition was inevitable.

For measuring the basic properties of catalyst, the temperature-programmed desorption of CO_2 (CO_2-TPD) was used and the spectra are shown in Figure 4.1. Desorption peaks are due to the presence of basic sites with different strengths. The pure ZrO_2 support had no significant desorption peak. It could be referred that it had no basic site. After loading 20%K on the ZrO_2 support, there was a desorption peak at 110°C. It could be attributed to the interaction of CO_2 with the site of the weak basic strength. From this result, it was observed that the basic strength increases with the KOH loading. In contrast, the pure mordenite support showed a desorption peak at 140°C, which is attributed to the basic site of weak strength from the interaction of CO_2. After loading 20%K on the mordenite support, there was no considerable desorption peak on its spectrum. Wang *et al.* (2001) proposed that there was another technique to examine the total basicity of catalyst such as the titration method.

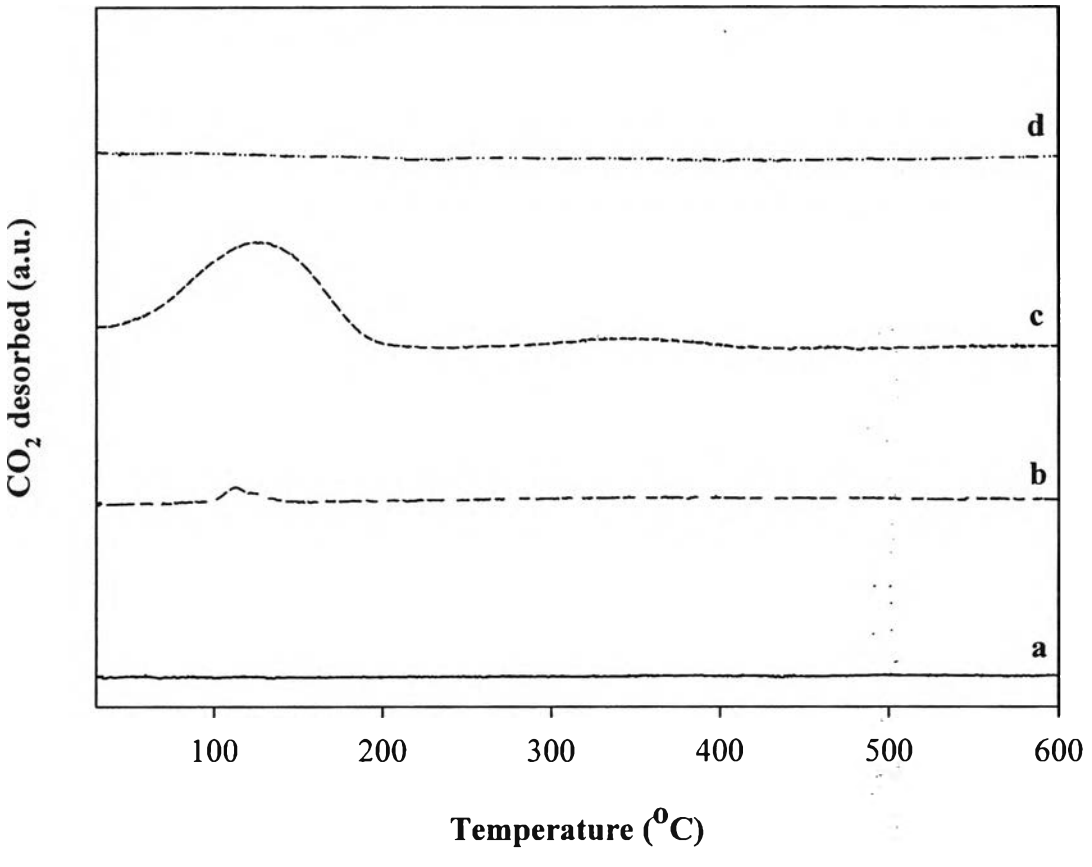

Figure 4.1 CO_2-TPD spectra of (a) ZrO_2, (b) 20%K/ZrO_2, (c) mordenite, and (d) 20%K/mordenite.

The calculated basicity from CO_2-TPD and titration methods are shown in Table 4.1. From this result, the basicity from CO_2-TPD is less than that from titration method. This is because the basic species of an overlapping structure were covered by upper layers and were not exposed to CO_2, but would react with an acidic agent if the top layers were resolved in an aqueous titration process. Consequently, the data of CO_2-TPD only designate the amount of basic sites exposed at the top of the overlapped structure while the titration data represents the total basicity of the composite (Wang *et al.*, 2001). From this reason, it is possible to propose that 20%K/mordenite also had the basic site, although it did not show any significant desorption peak from CO_2-TPD method.

Table 4.1 Characterization of pure support and loading catalyst

Type of catalyst	Basicity (mmol/g)		Surface area (m^2/g)	Percent K (element)
	CO_2-TPD	Titration		
ZrO_2	0.000	0.006	5.431	0
20%K/ZrO_2	0.066	5.007	5.166	10.22
Mordenite	0.640	0.718	315.5	0
20%K/Mordenite	0.070	5.163	3.547	9.23

The specific surface areas of the pure supports and potassium loaded catalysts are shown in Table 4.1. After loading with 20%K, the surface area of potassium loaded on ZrO_2 catalyst does not show significant difference as compared to the pure support. In other side, the significant decrease of surface area was observed for mordenite, which possess a one-dimensional 12-ring pore system and could be blocked by the incorporation of potassium oxide species (Ramos *et al.*, 2008). Moreover, loading with potassium may lead to the modification of mordenite structure, which would be another reason of the obvious decrease in surface area. Although the loaded catalyst had lower surface area than the support, the presence of potassium on ZrO_2 and mordenite support enhanced the basic sites of the catalysts and subsequently improved their catalytic activity (Longloilert, 2008).

The potassium content was identified by the Energy Dispersive Spectrometer (EDS). Table 4.1 also shows the potassium contents of both pure supports and potassium loaded catalysts. This result confirmed that the impregnation of 20%K caused a modification of chemical composition of the pure support. The increasing concentration of potassium element led to the decreasing of surface area and the increasing of basicity.

The scanning electron microscope has extensively been used to examine the morphology of catalysts. Figure 4.2 shows the SEM micrographs of the pure support and loaded catalyst. The results showed that the particles of ZrO_2 support were agglomerated and had a spherical shape. After loading with 20%K, the particle size of the catalyst was increased. This is because the potassium species was highly distributed upon the surface and aggregated to form the higher particle size. That led

to the decreasing of surface area of catalyst, which was supported by the BET surface area results. For mordenite support, it also had an obvious distribution of the potassium species on the surface. That led to a good dispersion of potassium on mordenite support, which was important for reaction. This result corresponded to the potassium content measured by EDS.

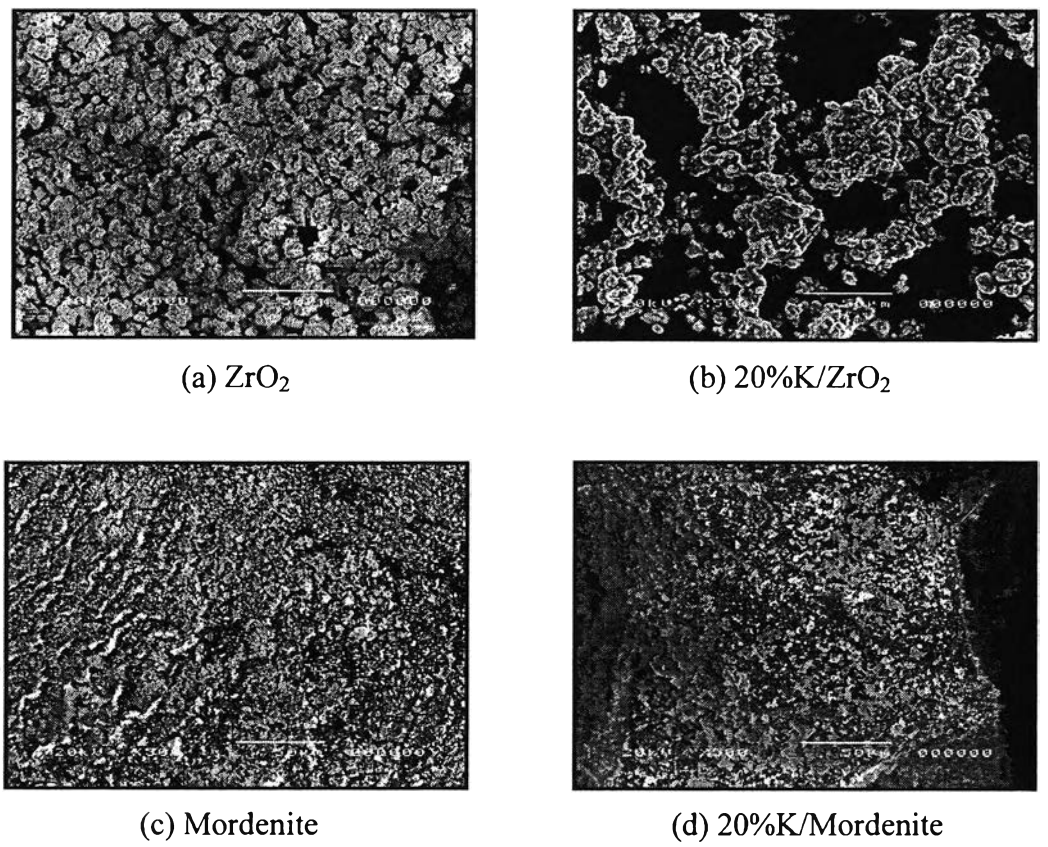

(a) ZrO_2 (b) 20%K/ZrO_2

(c) Mordenite (d) 20%K/Mordenite

Figure 4.2 SEM micrographs of pure supports and loading catalysts at 500× magnification.

The Fourier Transform Infrared Spectrophotometer (FTIR) was used to identify the functional groups and structural features of a molecule (Coates, 2000). The FTIR spectra of pure supports and loading catalysts are shown in Figure 4.3. The absorption peaks of ZrO_2 sample essentially showed various stretching frequencies. The absorption peaks appeared at 445 and 410 cm^{-1} correspond to the doublet of coordinated water (Powers and Gray, 1973). There were some particular peaks

identified for ZrO_2 phases at 740 and 500 cm^{-1} due to Zr–O_2–Zr asymmetric and Zr–O stretching modes, respectively (Sahu and Rao, 2000).

After loading with KOH with impregnation method, there was a new broad band peak at 3300–3700 cm^{-1}, corresponding to O–H band of the physically absorbed water on molecule (Xie and Huang, 2006). Other new peaks appeared at 1550 and 1410 cm^{-1}, which is attributed to the vibrational mode of CO_3^{2-}. This carbonates were supposed to be formed by the reaction of K_2O with carbon dioxide during the calcination procedure in air (Xie and Li, 2006). It could be referred that after loading with KOH, there was a modification of the structure of ZrO_2 support.

For the pure mordenite support, the absorption peaks at 3614 and 3460 cm^{-1} were assigned to the OH–stretching associated to the terminal silanol groups (Salla, 2005). And the H–O–H frequency of the H_2O molecule was located at a wavenumber of 1629–1646 cm^{-1} with a medium intensity. The set of strong intensity peaks at 1224 and 1046 cm^{-1} were ascribed to the vibration of external TO_4 (T = Al, Si) and the antisymmetrical stretching vibration of the tetrahedral (T–O bonds), respectively. The other group of absorption band around 628–789 cm^{-1} correspond to the characteristic vibration of the symmetrical stretching of Si (Al)–O bonds. And the bending of O–Si (Al)–O was interpreted at 437 cm^{-1} (Ostroumov and Corona-Chávez, 2003). These results showed the functional group and the characteristic of pure mordenite support.

The modified characteristic occurred in the K/mordenite catalyst. Many absorption peaks were transformed due to the loading of K. Evidently, the reduction of intensity of OH–stretching vibration at 3600 cm^{-1} occurred and changed to a broad band. In addition, the set of high intensity absorption peak around 1250–1000 cm^{-1} of pure mordenite support converted to a broad peak at 800–1300 cm^{-1}. It could be referred that the impregnated of KOH may have some effects on the structure and composition of mordenite zeolite support.

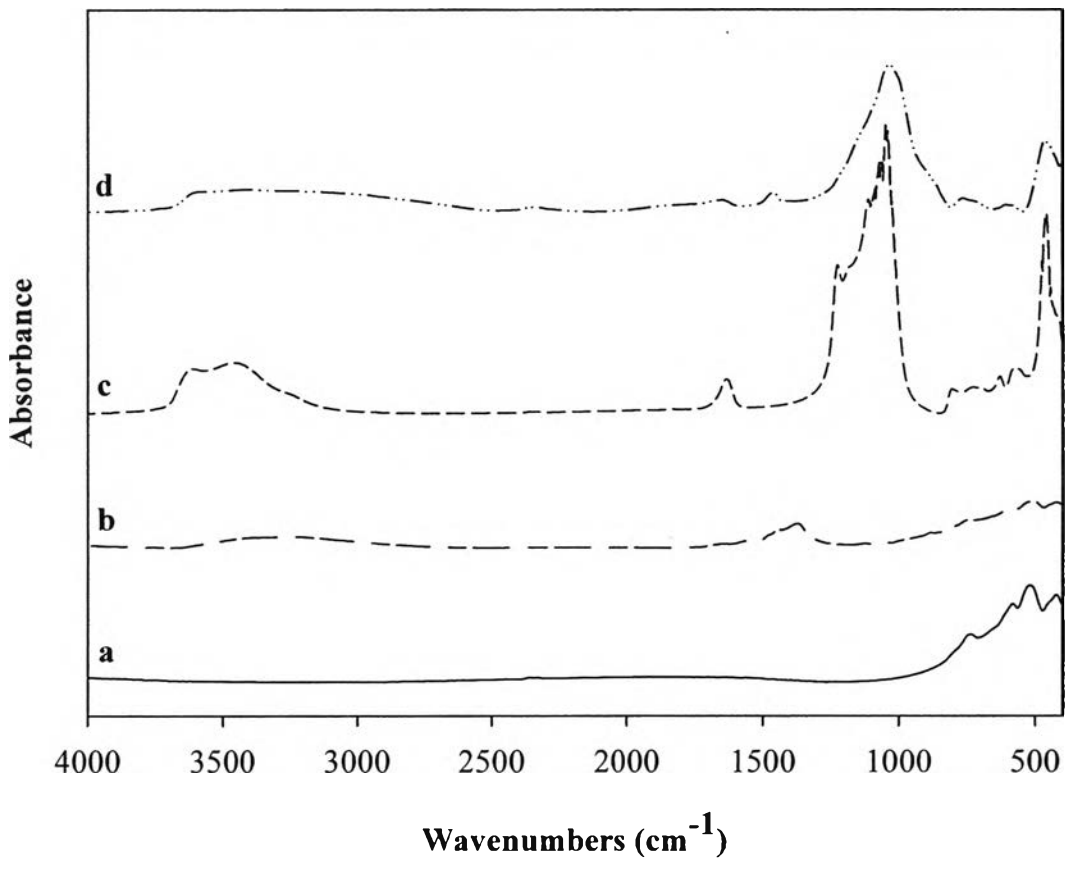

Figure 4.3 FTIR Spectra of (a) ZrO_2, (b) 20%K/ZrO_2, (c) mordenite, and (d) 20%K/mordenite.

The X-ray Diffraction (XRD) was used for identification and characterization of crystalline solids. As shown in Figure 4.4, the pure supports and loading catalysts were examined by means of XRD. The characteristic peaks of parent ZrO_2 were illustrated at 2θ = 28°, 31.5°, 34°, 49°, 50°, 54°, 55°, and 60°. This result corresponded to Wang *et al.* (2001). They proposed that there were two crystal phases formed in this parent ZrO_2, monoclinic baddeleyite and tetragonal form, and the former had stronger intensity than the latter. However, the tetragonal form was observed at 2θ = 50.2° and 60.2°. After impregnated KOH on ZrO_2 support, K/ZrO_2 catalyst had new characteristic peaks of K_2O as new phase. It was detected at 2θ = 20°, 24.5°, 31°, 45°, 47°, 55°, and 62°. This K_2O phase was the product of the KOH

decomposition to form strong basic sites, attributed to the high catalytic activity and basicity of the catalysts (Xie *et al.*, 2006).

On the other hand, the diffraction peaks at 2θ = 13.5°, 19.6°, 22.3°, 25.7°, 26.3°, 27.5°, and 30.9° were assigned to the crystallinity of pure mordenite support. Nevertheless, when KOH was loaded on the mordenite support, it changed the crystallinity of mordenite, as shown in Figure 4.4. There was no obvious diffraction peak because it has transformed into an amorphous structure. Zhu *et al.* (1999) proposed that loading with KOH on the zeolite led to an intensive interaction with the SiO_4 tetrahedra of the surface of host, so the structure of KOH/mordenite became amorphous, as shown in this result. Moreover, the result from the XRD pattern of K/mordenite catalyst agreed with the result from the FTIR spectra. They confirmed that the structure and crystallinity of K/mordenite catalyst was modified from the structure of pure mordenite support.

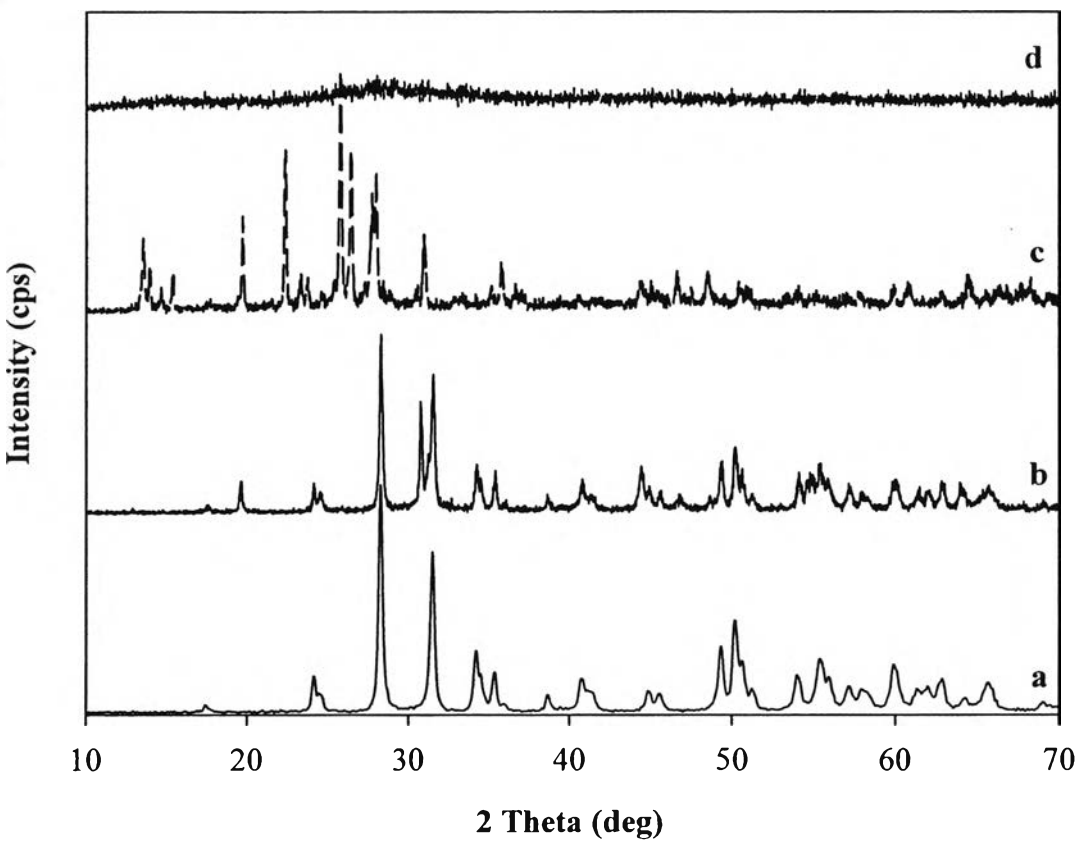

Figure 4.4 XRD patterns of (a) ZrO_2, (b) 20%K/ZrO_2, (c) mordenite, and (d) 20%K/mordenite.

4.2 Transesterification

The 20%K/ZrO_2 and 20%K/mordenite catalysts were studied as heterogeneous basic catalysts for the transesterification. To investigate the optimum conditions for the catalysts in the transesterification of palm oil, the starting conditions for the potassium hydroxide on the supports were set at a methanol-to-oil molar ratio of 15:1, a reaction temperature of 60°C, 12 wt% of the catalyst (based on the weight of the vegetable oil), and a feed flow rate of 11 ml/min.

4.2.1 Influence of Reaction Time on Methyl Ester Content

The dependence of the methyl ester content on the reaction time was studied in the presence of the KOH/ZrO_2 and KOH/mordenite catalysts with 40–50 mesh. The reaction time was varied at 2, 4, 6, and 8 hours. The characterization of biodiesel and spent catalysts were performed and the results are discussed.

4.2.1.1 Biodiesel Analysis

Two different techniques, Gas Chromatrography (GC) and Proton Nuclear Magnetic Resonance (^{1}H-NMR), were used to analyze the methyl ester content of biodiesel products. Figure 4.5 presents the variation of methyl ester content with different reaction times of 20%K/ZrO_2 catalyst. The results indicated that the methyl ester content initially increased with the reaction time from 2 to 6 hours and slightly decreased after 6 hours. The maximum methyl ester content of 95.29 wt% was obtained at 6 hours reaction time. In addition, both techniques were concurred in the same trend but the data from ^{1}H-NMR had lower methyl ester content about 3% compared to GC. Knothe (2001) proposed that GC to this date have been the most widely used method for the analysis of biodiesel due to its generally higher accuracy in quantifying minor components. So, it was possible to propose that the GC results had higher methyl ester content than the result from ^{1}H-NMR. By the way, the GC had some drawbacks such as it was a time-consuming method. Meanwhile, spectroscopic method such as ^{1}H-NMR was faster and simpler than chromatographic ones. The yield of methyl esters was calculated by comparing the peak area of methoxy and methylene protons. However, instrumentation and maintenance costs

were relatively high and were the main drawback of the ^{1}H-NMR technique (Monteiro *et al.*, 2008).

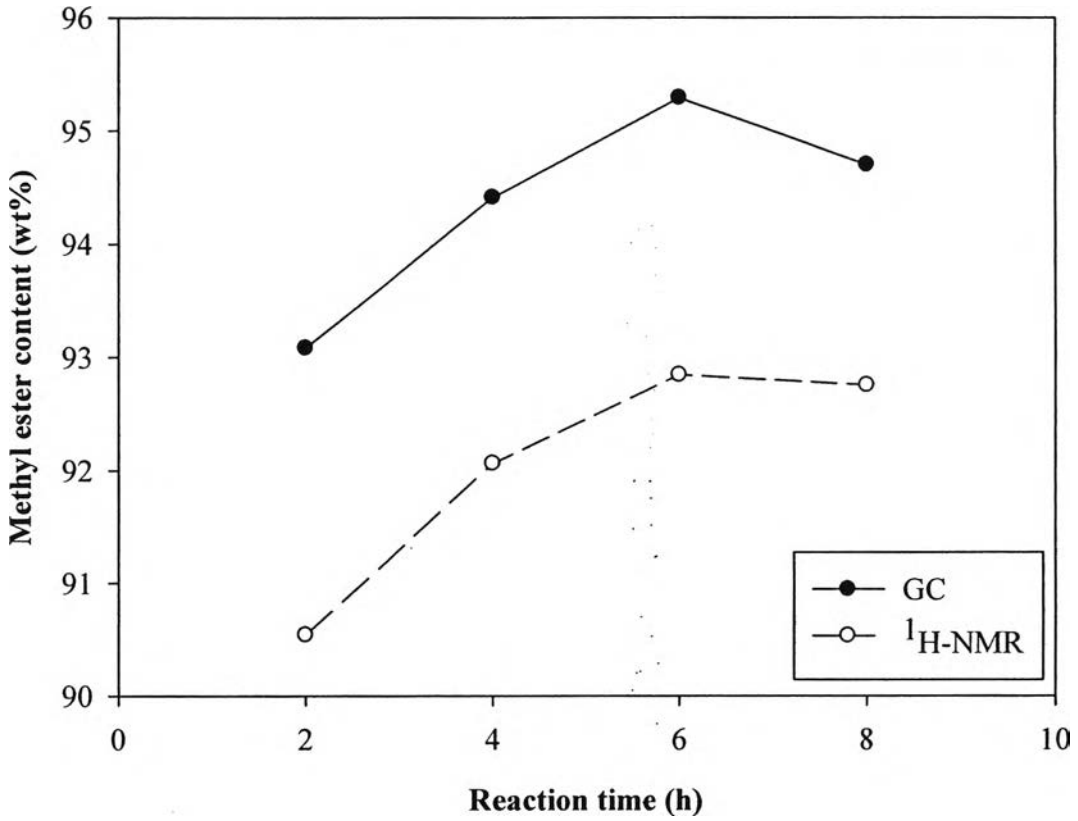

Figure 4.5 Methyl ester content as a function of reaction time. Reaction conditions: KOH/ZrO_2 catalyst amount 12 wt%; a catalyst particle size of 40–50 mesh; a methanol-to-oil molar ratio of 15:1; a reaction temperature of 60°C; and a flow rate of 11 ml/min.

The influence of reaction time on the methyl ester yield of 20%K/mordenite catalyst are illustrated in Figure 4.6. The methyl ester content was increased in the reaction time range between 2 and 4 hours, thereafter remained nearly steady, and lessened in the range between 6 and 8 hours; the maximum methyl ester content of 94.54 wt% was achieved at 4 hours reaction time. Moreover, GC and ^{1}H-NMR results also showed in the same tendency.

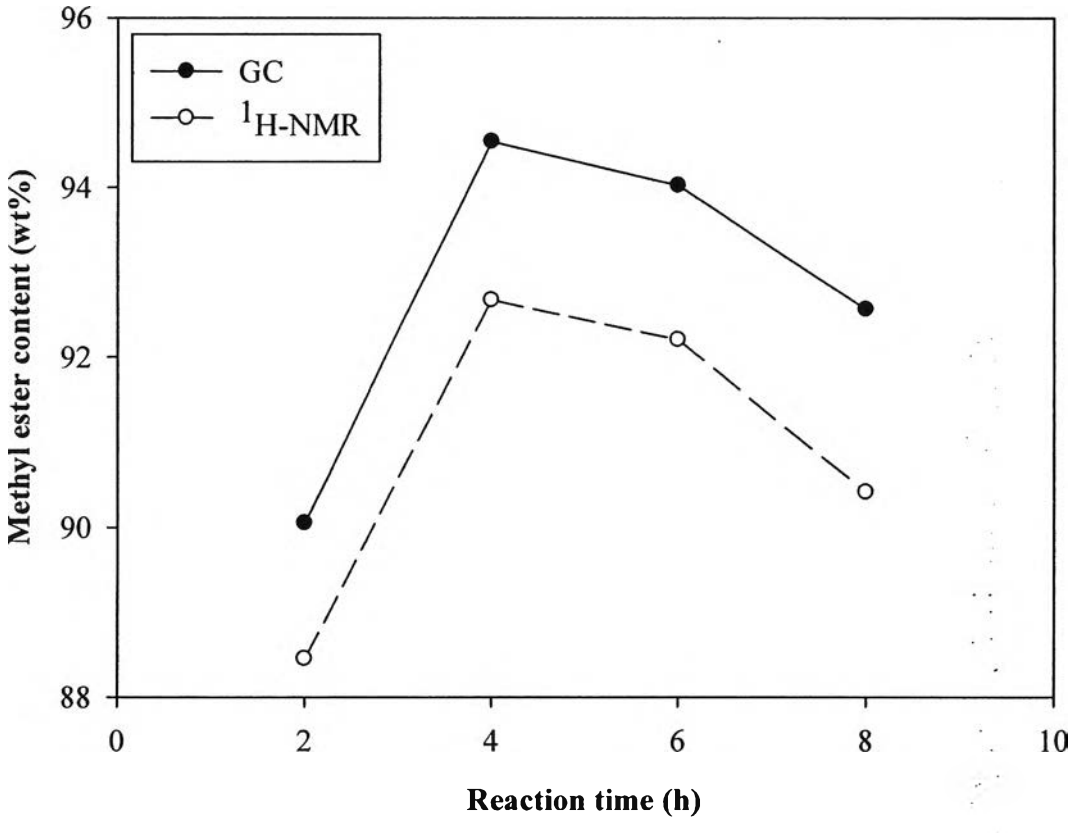

Figure 4.6 Methyl ester content as a function of reaction time. Reaction conditions: KOH/mordenite catalyst amount 12 wt%; a catalyst particle size of 40–50 mesh; a methanol-to-oil molar ratio of 15:1; a reaction temperature of 60°C; and a flow rate of 11 ml/min.

4.2.1.2 Catalyst Characterization

The fresh and spent catalysts without pretreatment from various reaction times were characterized by many methods.

The FTIR spectra of the fresh and spent K/ZrO_2 catalysts with various reaction times are shown in Figure 4.7. From this result, it is clearly observed that spent catalysts had new absorption peaks at 2922 cm^{-1}, which were assigned to the C–H stretching modes. Two peaks appeared at 1740 and 1160 cm^{-1} were due to the stretching absorption of aldehyde (C=O) and ester (C–O), respectively. Two alkanes peaks which was attributed the bending absorption of methylene (CH_2) and methyl (CH_3) groups appeared at 1465 and 1375 cm^{-1}, respectively (Yunus *et al.*,

2009). All these peaks showed the characteristic of oil, so it could be referred that the spent catalyst had the deposition of oil upon the surface. Moreover, the absorption peaks of spent catalyst with various reaction times were not significantly difference.

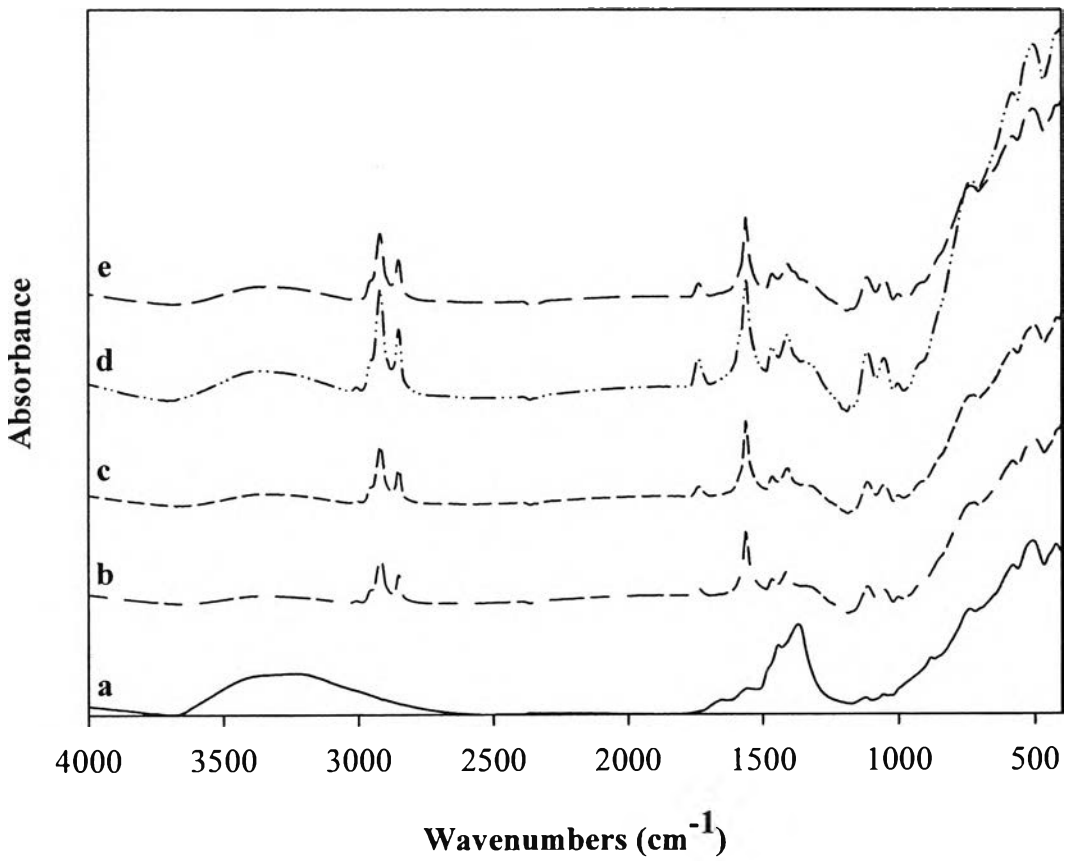

Figure 4.7 FTIR Spectra of fresh 20%K/ZrO_2 (a), spent catalysts from 2 (b), 4 (c), 6 (d), and 8 (e) hours of reaction time. Reaction conditions: KOH/ZrO_2 catalyst amount 12 wt%; a catalyst particle size of 40–50 mesh; a methanol-to-oil molar ratio of 15:1; a reaction temperature of 60°C; and a flow rate of 11 ml/min.

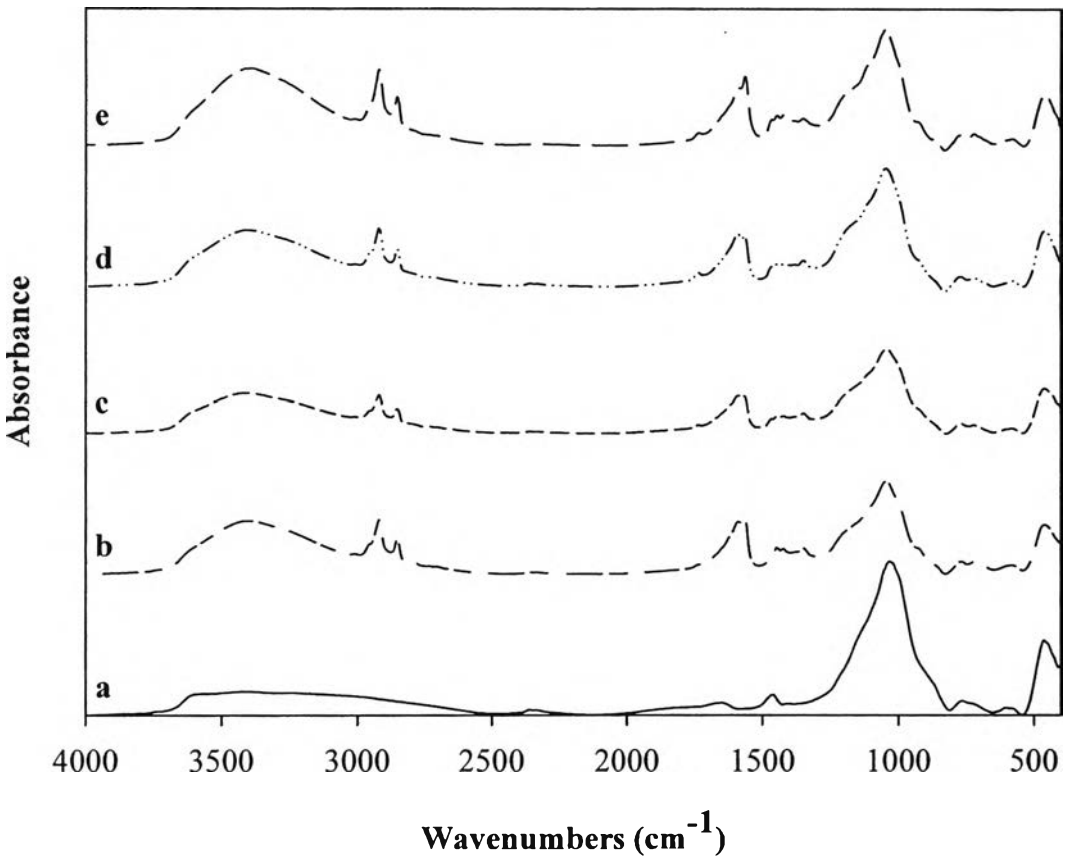

Figure 4.8 FTIR Spectra of fresh 20%K/mordenite (a), spent catalysts from 2 (b), 4 (c), 6 (d), and 8 (e) hours of reaction time. Reaction conditions: KOH/mordenite catalyst amount 12 wt%; a catalyst particle size of 40–50 mesh; a methanol-to-oil molar ratio of 15:1; a reaction temperature of 60°C; and a flow rate of 11 ml/min.

Figure 4.8 illustrates the FTIR spectra of fresh and spent K/mordenite catalysts with various reaction times. The spent catalysts also showed new absorption peaks as a result of the oil deposition during the reaction. The new peaks were found at 2922, 1740, and 1160 cm^{-1}, which were described to the C–H, aldehyde (C=O), and ester (C–O), respectively. Other new peaks were observed at 1465 and 1375 cm^{-1}, which were assigned to the bending absorption of methylene (CH_2) and methyl (CH_3) groups. Moreover, the spent catalysts had a higher intensity of broad band peak at 3300–3700 cm^{-1}, which was corresponding to O–H band of the

physically absorbed water on molecule (Xie and Huang, 2006). From these FTIR spectra, it could be referred that the spent catalysts with various reaction times might have the similar structure because all of them showed the new absorption peaks from oil deposition. Nevertheless, the peaks of mordenite support still appeared on the spent catalysts spectra.

The Scanning Electron Microscope (SEM) results showed the morphology and surface structure of the fresh and spent catalysts with various reaction times, as shown in Figure 4.9. The results showed that all catalysts were almost spherical in shape, although the particle size of the spent K/ZrO_2 catalyst was larger than the fresh one. It could be explained that the refined palm oil (a raw material of transesterification) has been deposited onto the catalyst particles with increasing reaction time (Park *et al.*, 2008). However, the morphology of spent catalysts from the four different reaction times were almost identical.

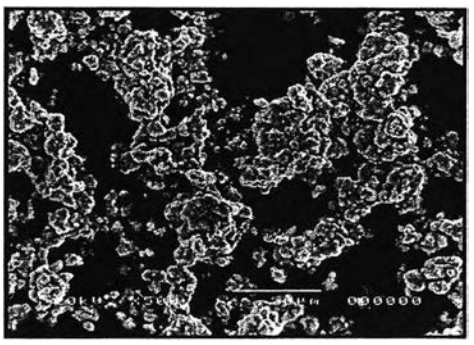

(a) Fresh 20%K/ZrO_2

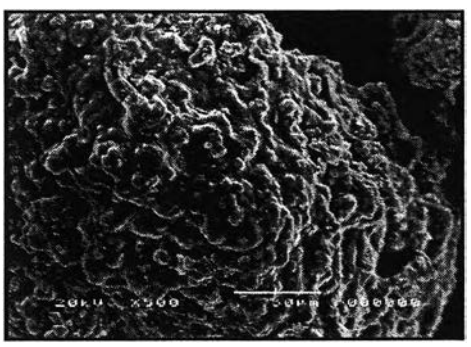

(b) Spent K/ZrO_2
from 2 hours reaction time

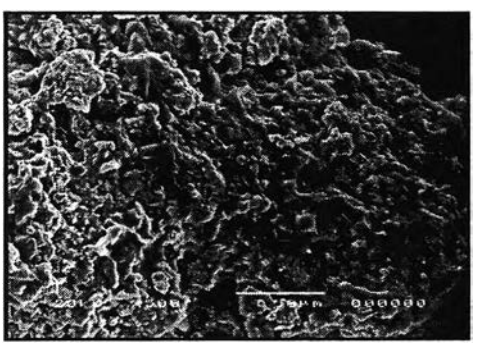

(c) Spent K/ZrO_2
from 4 hours reaction time

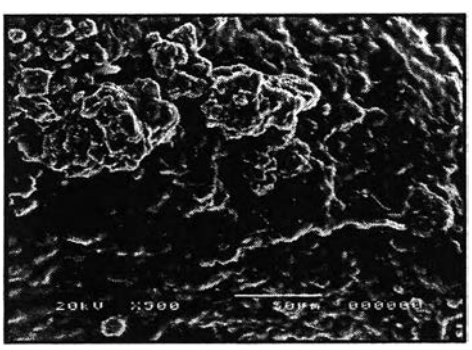

(d) Spent K/ZrO_2
from 6 hours reaction time

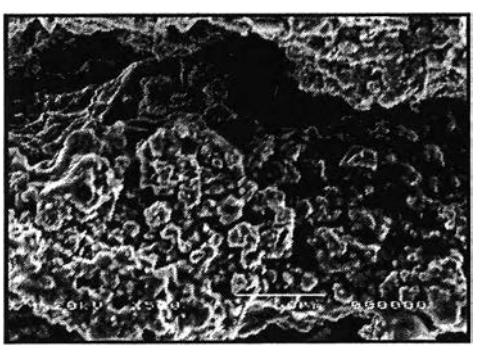

(e) Spent K/ZrO_2
from 8 hours reaction time

Figure 4.9 SEM micrographs of fresh and spent catalysts with various reaction time at 500× magnification. Reaction conditions: KOH/ZrO_2 catalyst amount 12 wt%; a catalyst particle size of 40–50 mesh; a methanol-to-oil molar ratio of 15:1; a reaction temperature of 60°C; and a flow rate of 11 ml/min.

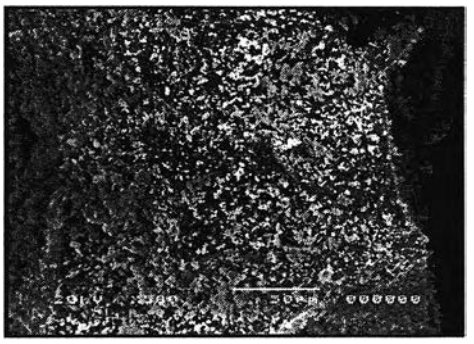

a) Fresh 20%K/mordenite

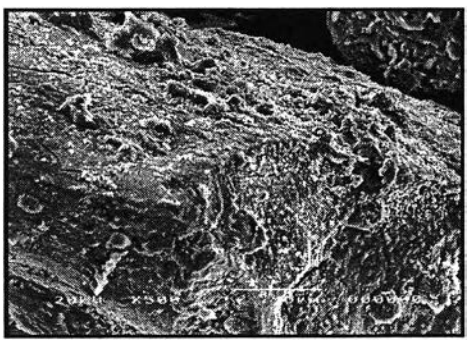

(b) Spent K/mordenite
from 2 hours reaction time

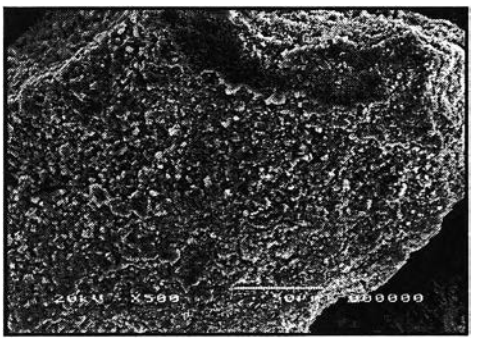

(c) Spent K/mordenite
from 4 hours reaction time

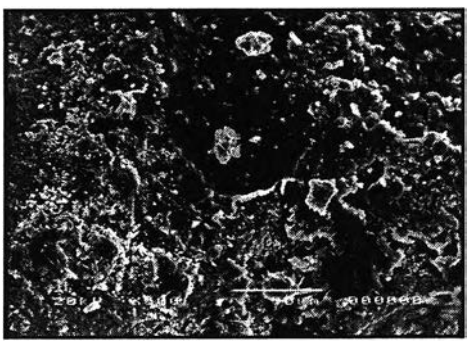

(d) Spent K/mordenite
from 6 hours reaction time

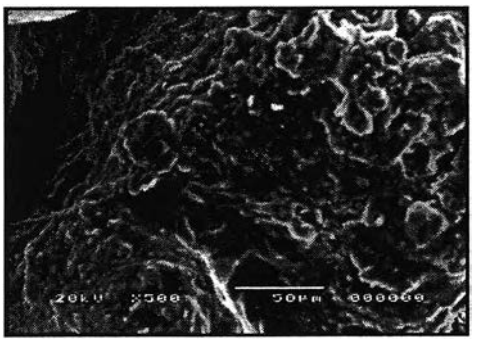

(e) Spent K/mordenite
from 8 hours reaction time

Figure 4.10 SEM micrographs of fresh and spent catalysts with various reaction time at 500× magnification. Reaction conditions: KOH/mordenite catalyst amount 12 wt%; a catalyst particle size of 40–50 mesh; a methanol-to-oil molar ratio of 15:1; a reaction temperature of 60°C; and a flow rate of 11 ml/min.

Figure 4.10 reveals the SEM micrographs of the fresh and spent K/mordenite catalysts with various reaction times. Evidently, the modification of surface structure of the spent catalysts has occurred comparing to the fresh catalysts. The exterior surface of fresh catalyst had no agglomeration, but all of the spent catalysts had. Because of the oil deposition onto the surface of the spent catalyst, it led to the agglomeration and coverage of active species.

The Energy Dispersive Spectrometer (EDS) was used to examine the potassium content on the surface of the catalysts, as shown in Table 4.2. The fresh catalysts (20%K/ZrO_2 and 20%K/mordenite) had the highest potassium content. After the reaction, the potassium content of spent catalysts decreased compared to the fresh catalyst, implying that the active species was leached from the solid support during the reaction. Furthermore, the 6-hour spent K/ZrO_2 and the 4-hour spent K/mordenite catalysts had the lowest potassium content. Meanwhile, they yielded the highest methyl ester content of the product. From this result, it could be assumed that spent catalysts that was the highest leaching of potassium content, provided the highest conversion to biodiesel.

Table 4.2 Potassium content of the fresh and spent catalysts with various reaction times

Type of catalyst	K/ZrO_2		K/Mordenite	
	Percent K (element)	% Leaching	Percent K (element)	% Leaching
Fresh catalyst	10.22	-	9.23	-
Spent catalyst (2 hours)	10.06	1.57	7.88	14.63
Spent catalyst (4 hours)	7.54	26.22	3.75	59.37
Spent catalyst (6 hours)	7.47	26.91	4.86	47.35
Spent catalyst (8 hours)	7.49	26.71	6.23	32.50

4.2.2 Influence of Catalyst Particle Size on Methyl Ester Content

The dependence of the methyl ester content on catalyst particle size was investigated in the presence of the 20%K/ZrO_2 and 20%K/mordenite catalysts with the optimum reaction time of 6 and 4 hours, respectively. The catalyst particle size was varied at 40–50, 20–40, and less than 20 mesh. Biodiesel and spent catalysts were characterized to clarify the obtained results.

4.2.2.1 Biodiesel Analysis

GC and ^{1}H-NMR were also utilized for the analysis of biodiesel. The results are illustrated in Figure 4.11, which indicate the methyl ester content via the variation of catalyst particle size. For the 20%K/ZrO_2 catalyst, the highest methyl ester content of 95.29 wt% was achieved at a 40–50 mesh, which was the smallest size. Moreover, the bigger catalyst particle size led to the lower methyl ester content. Because the smaller catalyst particle size had more surface area, it provides a better contact between the reactants and the solid catalyst, especially for

the fixed-bed reactor. The reaction can occur easily and give a higher methyl ester content. In addition, the results from GC and ^{1}H-NMR were also presented in the same way.

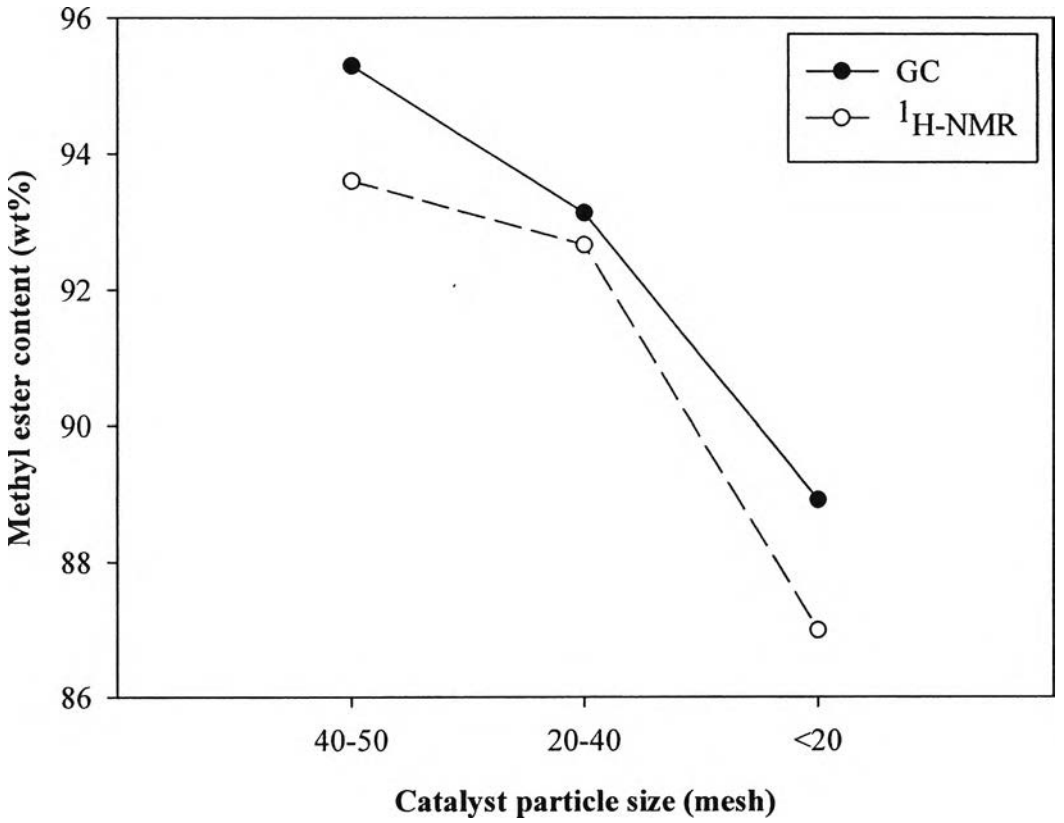

Figure 4.11 Methyl ester content as a function of catalyst particle size. Reaction conditions: KOH/ZrO_2 catalyst amount 12 wt%; a reaction time of 6 hours; a methanol-to-oil molar ratio of 15:1; a reaction temperature of 60°C; and a flow rate of 11 ml/min.

The effect of catalyst particle size of the 20%K/mordenite on the methyl ester yield was also investigated. In Figure 4.12, the methyl ester content versus catalyst particle size is presented. It could be seen that the methyl ester content decreased with the bigger catalyst particle size. The maximum methyl ester content of 94.54 wt% was obtained at the 40–50 mesh of catalyst particle size, which was the smallest size. This result agrees with the result of 20%K/ZrO_2 catalyst and the trend of GC and ^{1}H-NMR techniques were identical.

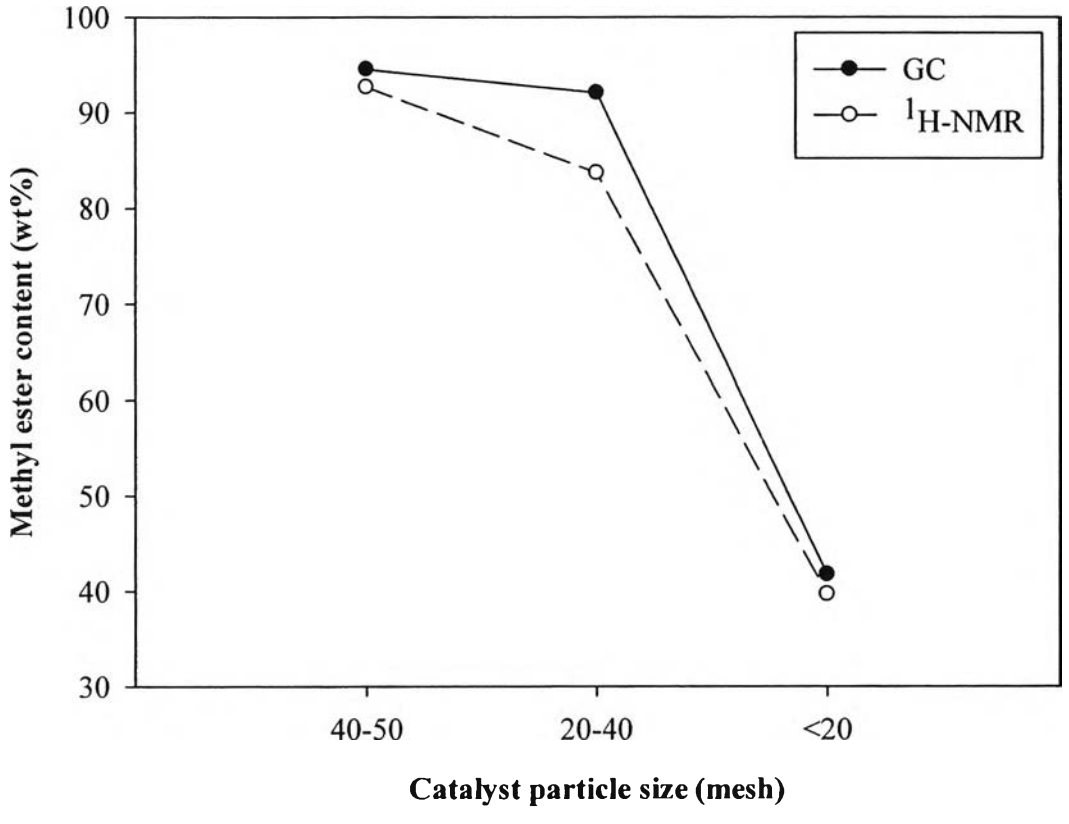

Figure 4.12 Methyl ester content as a function of catalyst particle size. Reaction conditions: KOH/mordenite catalyst amount 12 wt%; a reaction time of 4 hours; a methanol-to-oil molar ratio of 15:1; a reaction temperature of 60°C; and a flow rate of 11 ml/min.

4.2.2.2 Catalyst Characterization

The characterization of fresh and spent catalysts without pretreatment from various catalyst particle sizes were performed by many techniques.

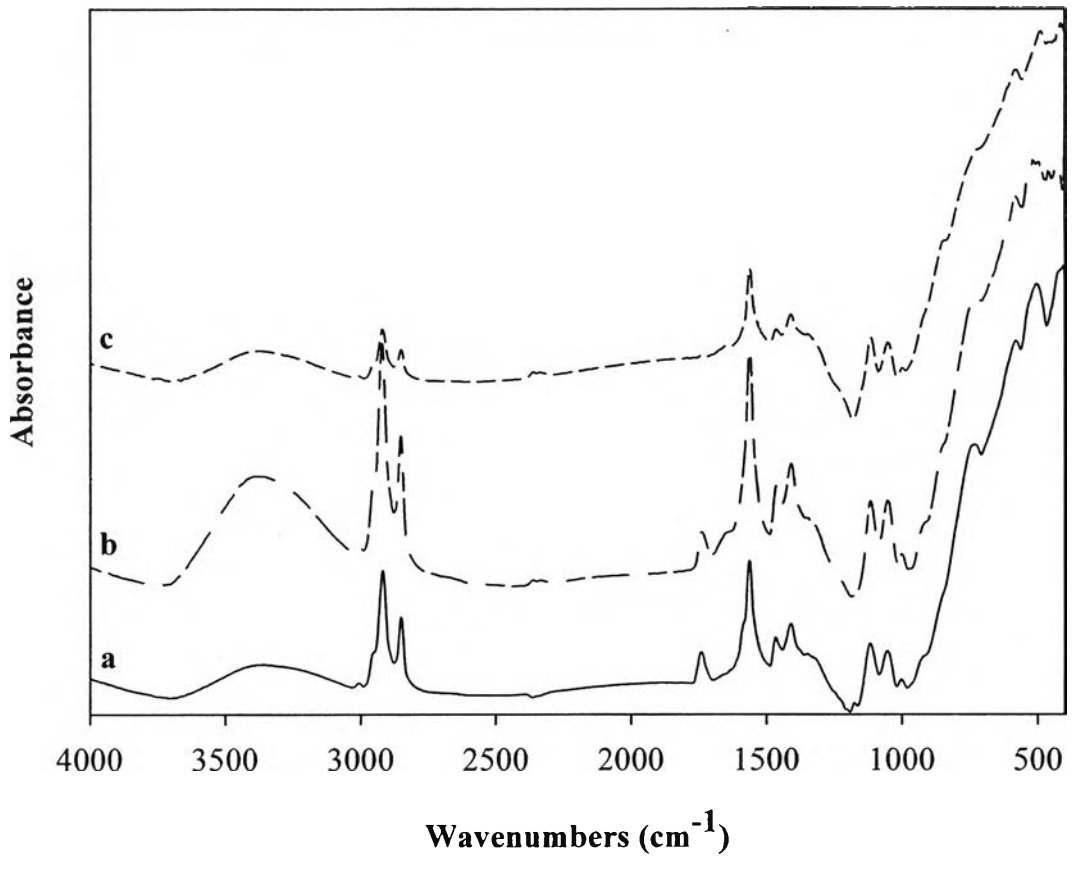

Figure 4.13 FTIR spectra of spent K/ZrO_2 catalysts with various catalyst particle size of (a) 40–50 mesh, (b) 20–40 mesh, and (c) Less than 20 mesh. Reaction conditions: KOH/ZrO_2 catalyst amount 12 wt%; a reaction time of 6 hours; a methanol-to-oil molar ratio of 15:1; a reaction temperature of 60°C; and a flow rate of 11 ml/min.

The Fourier Transform Infrared Spectrophotometer (FTIR) results are shown in Figure 4.13. All of spent K/ZrO_2 catalysts with various catalyst particle sizes presented the same absorption peaks of oil deposited on the surface from reaction. In addition, three catalyst particle sizes gave the similar trend of FTIR spectra. However, there were some distinctions at the intensity of the absorption peaks that referred to the different contents of oil deposition. Although, the catalyst particle size of 20–40 mesh showed the high intensity of absorption peak, it would not gave the higher methyl ester content, as for the result of biodiesel analysis.

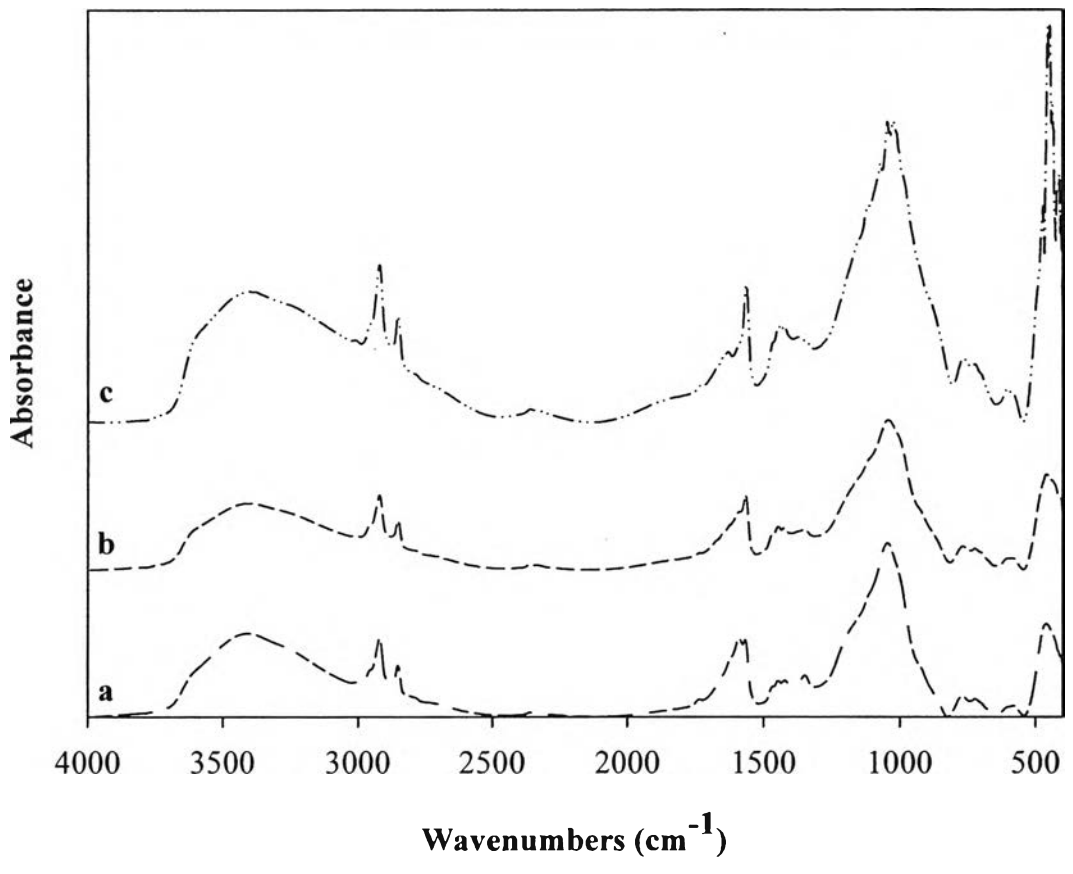

Figure 4.14 FTIR spectra of spent K/mordenite catalysts with various catalyst particle size of (a) 40–50 mesh, (b) 20–40 mesh, and (c) Less than 20 mesh. Reaction conditions: KOH/mordenite catalyst amount 12 wt%; a reaction time of 4 hours; a methanol-to-oil molar ratio of 15:1; a reaction temperature of 60°C; and a flow rate of 11 ml/min.

Figure 4.14 illustrates the FTIR spectra of spent K/mordenite catalysts with various catalyst particle sizes. Three types of catalyst particle size gave the similar spectra, implying to the deposition of oil onto the surface. For the intensity of absorption peaks, the catalyst with the particle size less than 20 mesh, which was the biggest size, had the higher intensity compared to others. Nevertheless, the methyl ester content of the catalyst with the particle size less than 20 mesh was the lowest.

The Scanning Electron Microscope (SEM) results showed the morphology of the various catalyst particle sizes of 20%K/ZrO_2 spent catalysts without pretreatment, as shown in Figure 4.15. The results exhibited that the surface structures of three different spent catalyst particle sizes were slightly similar. The distribution of potassium that was loaded onto the support and the refined palm oil that deposited onto the catalyst particles led to the rough surface of catalysts. In addition, the significant distinction of catalyst particle sizes led to the different morphology with the same at 500× magnification of SEM micrographs.

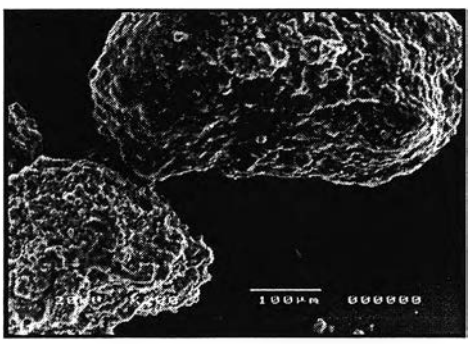

(a) Spent K/ZrO_2, 40–50 mesh

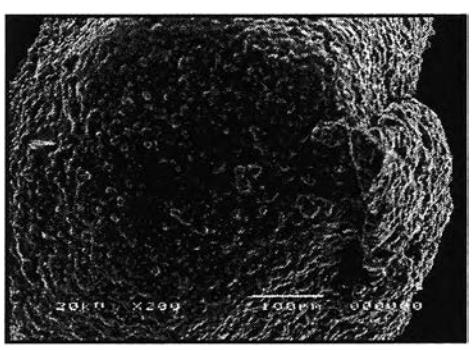

(b) Spent K/ZrO_2, 20–40 mesh

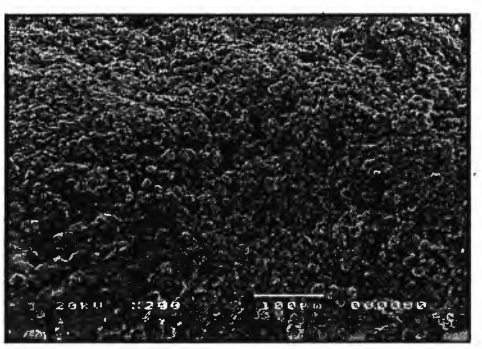

(c) Spent K/ZrO_2, <20 mesh

Figure 4.15 SEM micrographs of spent K/ZrO_2 catalysts without pretreatment at 500× magnification. Reaction conditions: KOH/ZrO_2 catalyst amount 12 wt%; a reaction time of 6 hours; a methanol-to-oil molar ratio of 15:1; a reaction temperature of 60°C; and a flow rate of 11 ml/min.

For the spent 20%K/mordenite catalyst with different particle sizes, the surface structure was illustrated by SEM micrographs in Figure 4.16. The morphology and the exterior surface structure of various catalyst particle sizes were insignificantly related. Although, all of them had the rough surfaces from the potassium loading and the deposition of refined palm oil, the morphology of catalysts were different. This was because the distinction of catalyst particle size led to the different morphology with the similarity of 500× magnification of SEM micrographs.

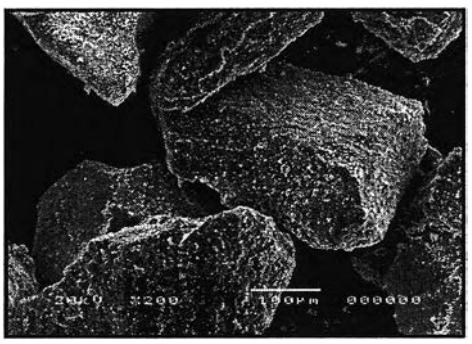

(a) Spent K/mordenite, 40–50 mesh

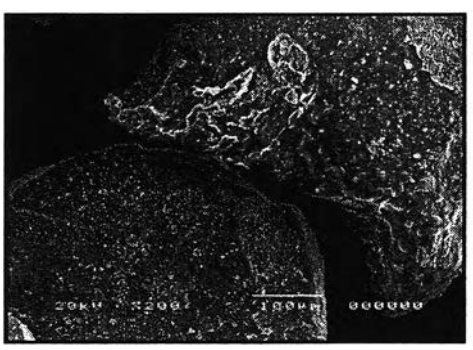

(b) Spent K/mordenite, 20–40 mesh

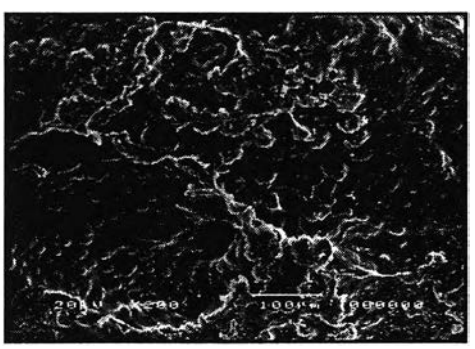

(c) Spent K/mordenite, <20 mesh

Figure 4.16 SEM micrographs of spent K/mordenite catalysts without pretreatment at 500× magnification. Reaction conditions: KOH/mordenite catalyst amount 12 wt%; a reaction time of 4 hours; a methanol-to-oil molar ratio of 15:1; a reaction temperature of 60°C; and a flow rate of 11 ml/min.

The potassium content was estimated by the Energy Dispersive Spectrometer (EDS). Table 4.3 shows the potassium content of the fresh and spent 20%K/ZrO_2 and 20%K/mordenite catalysts with various catalyst particle sizes. The results illustrated that the potassium content of the spent catalysts decreased compared to the fresh catalyst because the active species of catalyst was leached during reaction. In addition, two types of catalyst, K/ZrO_2 and K/mordenite, had a similar optimum catalyst particle size of 40–50 mesh. In this particle size range, it also gave the highest methyl ester content and the highest potassium leaching compared to other particle size range.

Table 4.3 Potassium content of the fresh and spent catalysts with various catalyst particle sizes

Type of catalyst	K/ZrO_2		K/Mordenite	
	Percent K (element)	**% Leaching**	**Percent K (element)**	**% Leaching**
Fresh catalyst	10.22	-	9.23	-
Spent catalyst (40–50 mesh)	7.47	26.91	3.75	59.37
Spent catalyst (20–40 mesh)	9.82	3.91	6.13	33.59
Spent catalyst (<20 mesh)	10.01	2.05	8.48	8.13

4.2.3 Stability of Catalyst in Transesterification

In order to study the stability of K/ZrO_2 and K/mordenite catalysts, the fresh catalyst with the optimum catalyst particle size was used for investigation. The reaction conditions were set at the optimum reaction time. After the first reaction (Cycle 1), the spent catalyst from the first run was instantly used for the second reaction (Cycle 2) with the same conditions but the reactants were changed to the new

one. The repeat reaction with the same spent catalyst was examined as the third reaction (Cycle 3).

The methyl ester content of three-cycle reaction was analyzed by GC compared with ^{1}H-NMR, as can be seen in Figure 4.17. As may be seen, a remarkable reduction in catalytic activity took place. For K/ZrO_2, the methyl ester content was dramatically decreased from 95.29 wt% in the first run to 7.56 wt% in the second run, and only 2.01 wt% for the last run. On the other hand, the methyl ester content of K/mordenite catalyst was gradually decreased from 94.54 wt% in the first run; 57.71 wt% for the second run, and 26.08 wt% in the last test. The difference trend of result between two types of catalyst showed the distinction of their stability. The K/mordenite catalyst gave higher reusability than the K/ZrO_2 catalyst. However, both catalysts illustrated the reduction of activity when using the same catalyst without any pretreament. Alonso *et al.* (2007) proposed that this decay could be due to two causes: (i) deactivation of active sites due to their poisoning by some molecule present in the reaction mixture; and (ii) a leaching of the active phase which the catalyst would have a smaller number of active sites in successive runs. To elucidate the first hypothesis of them, the regeneration of catalyst was attractive to further study.

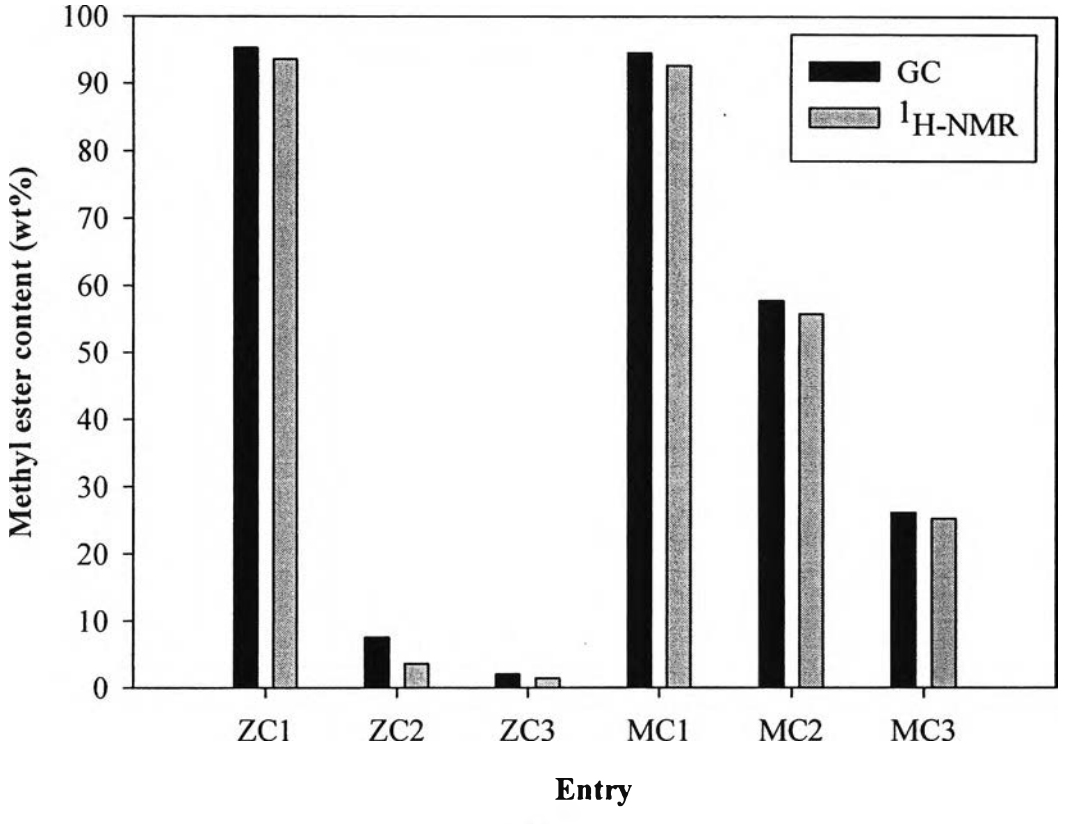

Figure 4.17 Methyl ester content as a function of run numbers of catalyst without pretreatment. (ZC: K/ZrO_2 with no. of cycle, MC: K/mordenite with no. of cycle) Reaction conditions: a methanol-to-oil molar ratio of 15:1; a reaction temperature of 60°C; a flow rate of 11 ml/min; a catalyst amount 12 wt% with 40–50 mesh; and a reaction time of 6 and 4 hours for KOH/ZrO_2 and KOH/mordenite catalyst, respectively.

4.2.4 Regeneration of Catalyst

As for the result of reusability of catalyst in 4.2.3, this indicated to the activity loss and the deactivation of the catalysts due to the potassium leaching or the blocking of the active sites by the products (Tittabut and Trakarnpruk, 2008). The regeneration process could be applied to reverse the deactivation. If the biodiesel product covers and blocks the active sites of catalyst, the oil washing will enhance the catalytic activity. Acetone was one of the most widely used industrial solvents, low in toxicity and did not cause adverse health or environmental effects at levels typically found in the workplace. In addition, acetone could be used as a solvent for oil

extraction (Johnson and Lusas, 1983). From these reasons, the catalyst regeneration by means of washing the spent catalysts with acetone was an attractive method.

4.2.4.1 Catalyst Characterization

The spent catalyst was regenerated by flowing acetone through the fixed-bed reactor and the acetone was removed out by drying at 110°C for 24 hours. To investigate the structure and morphology of the spent catalyst after treating, many techniques were utilized.

Figure 4.18 illustrates the FTIR spectra of fresh, spent (cycle 1), and treated K/ZrO_2 catalyst. The regeneration of catalyst via flowing by acetone led to the disappear once of the absorption peaks at 2922 and 1740 cm^{-1}, as shown in the treated catalyst. It could be implied that acetone could wash the oil, which deposited upon the exterior surface of catalyst. Furthermore, the treated catalyst had a reduction of a broad peak at 3450 cm^{-1} compared to fresh and spent catalysts. This peak assigned to the stretching absorption of (O–H) due to the intermolecular hydrogen bonding for water. Because acetone and water are the polar components, they have the dissolution property. So, water is soluble in acetone. From these results, it could be implied that treating catalyst by acetone could remove oil and adsorbed water from the catalyst surface. Moreover, the FTIR spectra of the treated catalyst was similar to the fresh catalyst, implying the morphology of the treated catalyst was quite similar to the fresh one.

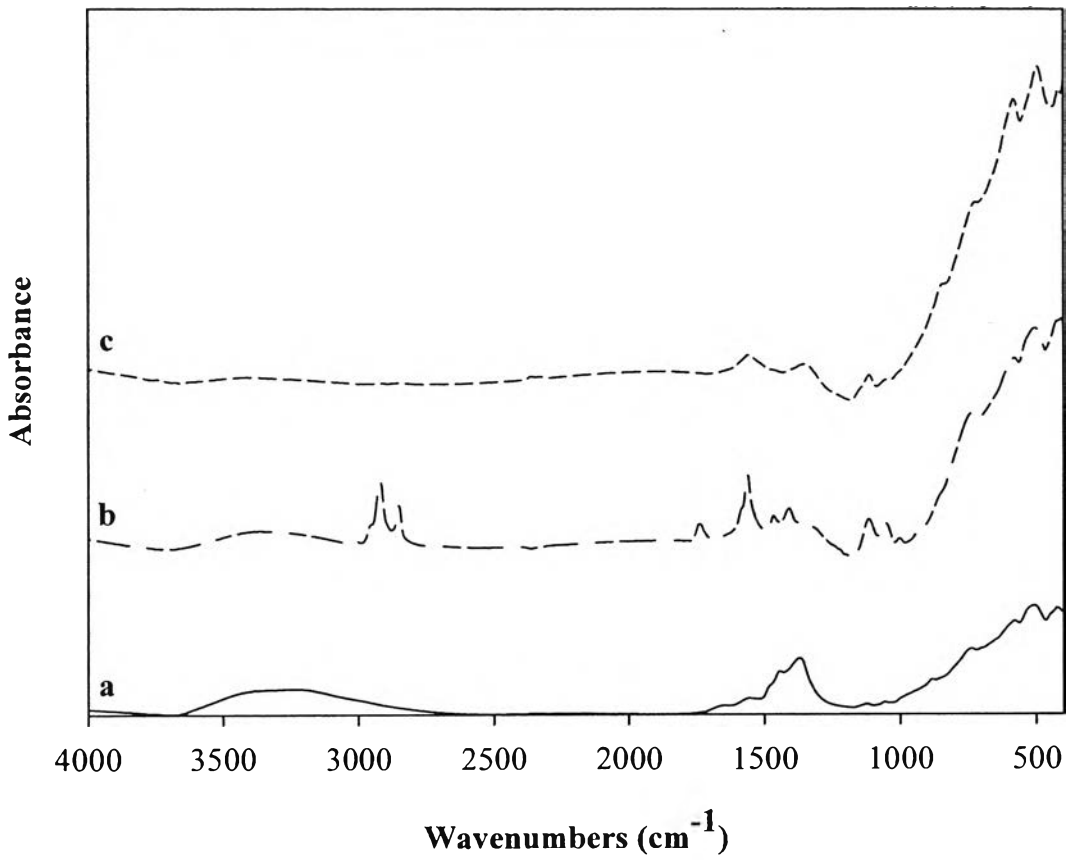

Figure 4.18 FTIR Spectra of (a) fresh 20%K/ZrO_2; (b) spent catalyst with optimum condition; and (c) treated catalyst with acetone.

The FTIR spectra of the fresh, spent (cycle 1), and treated K/mordenite catalyst are illustrated in Figure 4.19. It was clearly observed that the absorption peaks at 3450 cm^{-1} was decreased related to the removing oil from the surface of catalyst. In addition, the spectra of treated catalyst was similar to that of the fresh catalyst. It could be referred that after treating with acetone, the spent catalyst was recovered as the fresh catalyst.

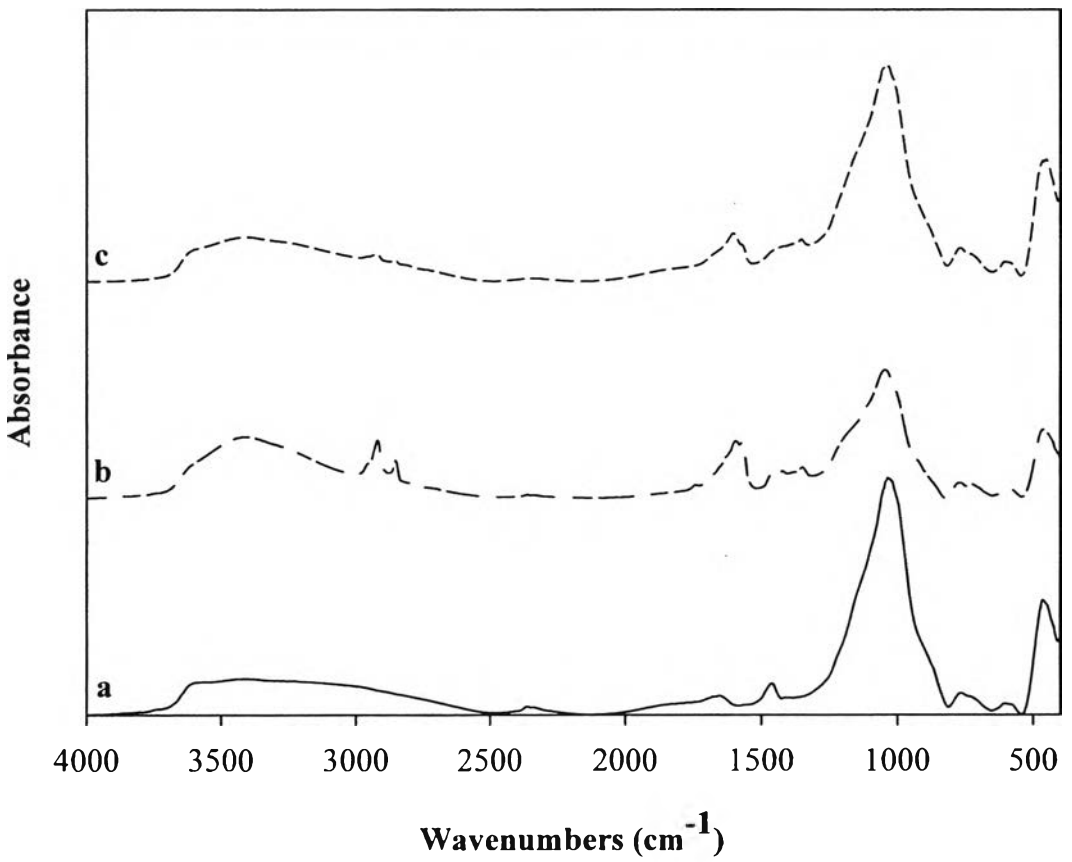

Figure 4.19 FTIR Spectra of (a) fresh 20%K/mordenite; (b) spent catalyst with optimum condition, and (c) treated catalyst with acetone.

The morphology and surface structure of the treated catalyst was characterized by the scanning electron microscope (SEM), as shown in Figure 4.20. For the K/ZrO_2 catalyst, the fresh catalyst was almost spherical in shape and had the smallest particle size, as compared to the other types. After reaction, the particle size of spent catalyst was increased and the surface structure was changed because the agglomeration of oil upon the exterior surface of the catalyst. After regeneration, the surface of treated catalyst was clearer than the spent one and the agglomeration of oil was disappeared. Because of flowing with acetone, it could wash the oil which, deposited upon the surface after reaction. This result agreed with the result from the FTIR.

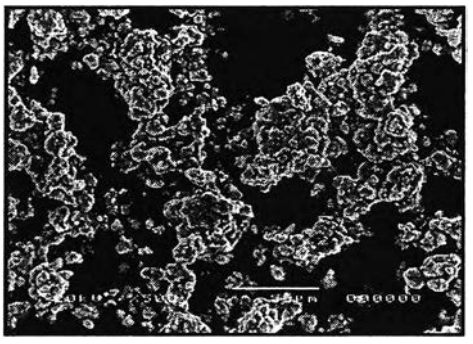

(a) Fresh 20%K/ZrO_2

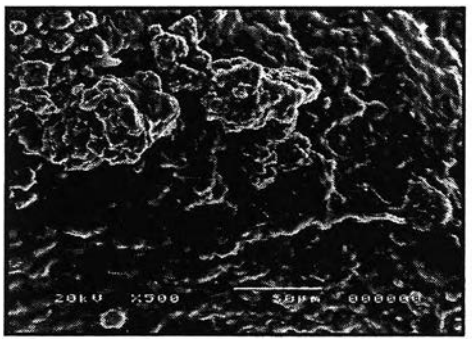

(b) Spent K/ZrO_2

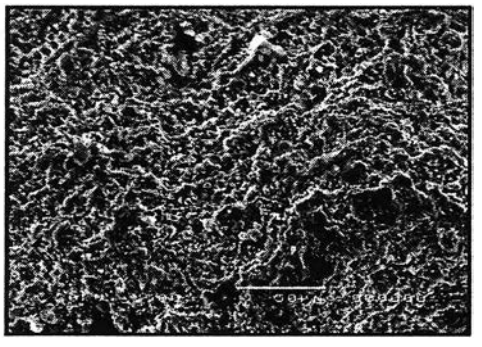

(c) Treated K/ZrO_2

Figure 4.20 SEM micrographs of fresh, spent and treated K/ZrO_2 catalysts with the optimum condition at 500× magnification.

Figure 4.21 shows the SEM micrographs of the fresh, spent, and treated K/mordenite catalysts. There was no apparent distinction between particle size and morphology of catalysts. On the other hand, the surface structure of the spent catalyst was transformed since the oil was deposited on the surface. For the treated catalyst, the regeneration with acetone destroyed the agglomeration of oil on the catalyst surface. And the surface structure became similar to the fresh one, implying to the related property of catalyst.

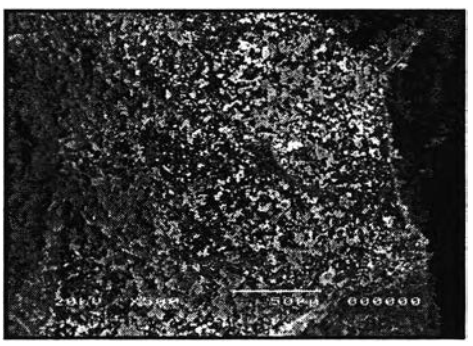

(a) Fresh 20%K/mordenite

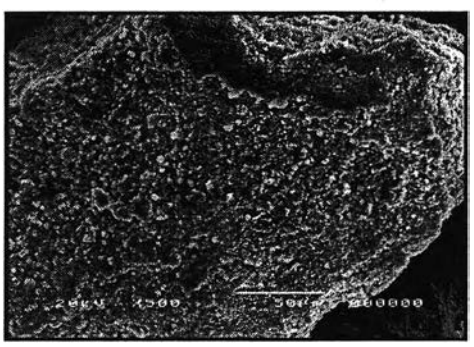

(b) Spent K/mordenite

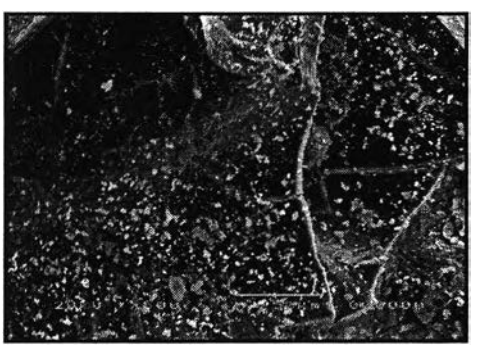

(c) Treated K/mordenite

Figure 4.21 SEM micrographs of fresh, spent and treated K/mordenite catalysts with the optimum condition at 500× magnification.

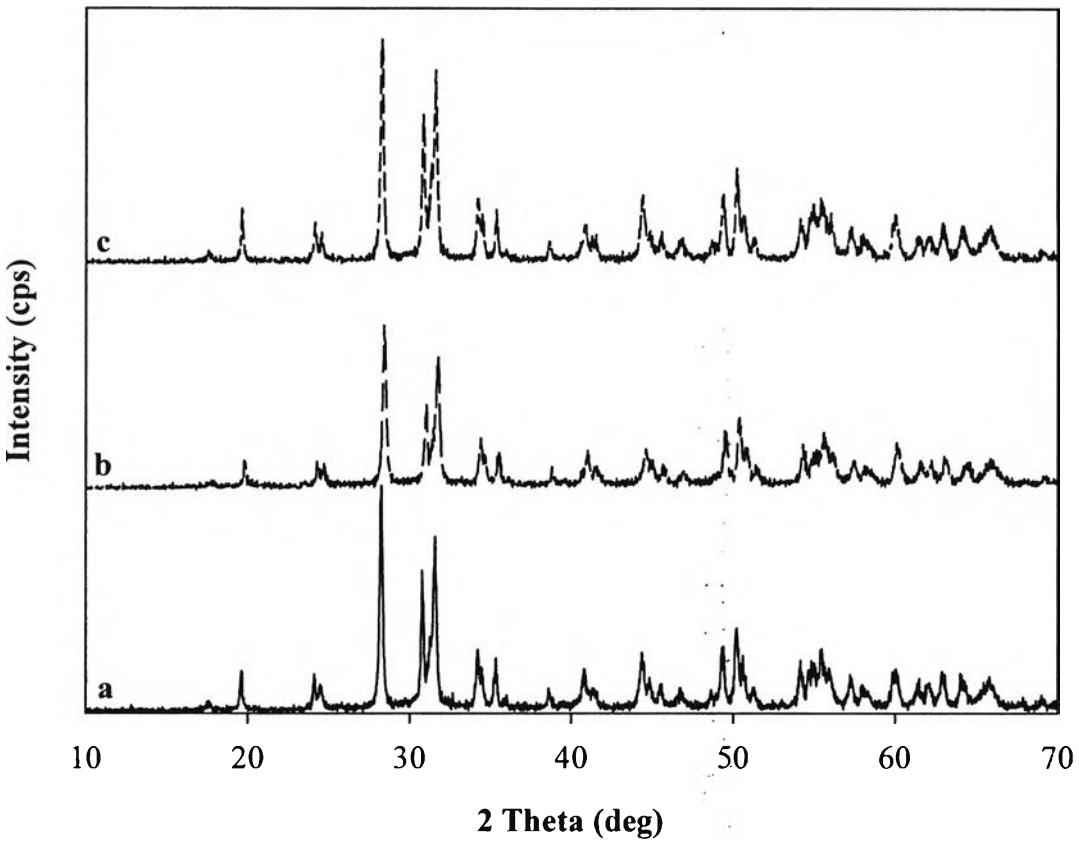

Figure 4.22 XRD patterns of (a) fresh 20%K/ZrO_2; (b) spent catalyst with optimum condition, and (c) treated catalyst.

The XRD patterns of the fresh, spent and treated K/ZrO_2 catalysts are displayed in Figure 4.22. The diffraction peaks of the spent catalyst shows no significant difference when compared to the fresh one. However, the intensity of K_2O was declined, which was easy detected at 2θ = 20°, 24.5°, 31°, 45°, 47°, 55° and 62°, especially for 2θ= 31°. The reduction of its intensity could be suggested that the active site might leach from the surface during the reaction (Iangthanarat, 2008). After catalyst regeneration, the characteristic XRD peaks of K_2O were increased, as shown in the result of treated catalyst. It might be supposed that acetone could wash the oil, which agglomerated upon the surface of catalyst. Moreover, the intensity of the K_2O active sites was higher because the catalyst pretreatment led to the recovery of active sites from using acetone. In addition, the

diffraction peaks of treated catalyst was similar to the fresh catalyst, implying to the recovery of characteristic after regeneration.

Figure 4.23 shows the XRD patterns of the fresh, spent and treated K/mordenite catalysts. All of them illustrated the identical diffraction peaks. There was no crystallinity and evidently diffraction lines, implying to the amorphous structure. Due to the modification of mordenite zeolite structure after loading with high content of KOH, the structures was transformed from crystal phase to amorphous phase. From this result, the XRD techniques was not suitable to identify the difference of three types K/mordenite catalyst.

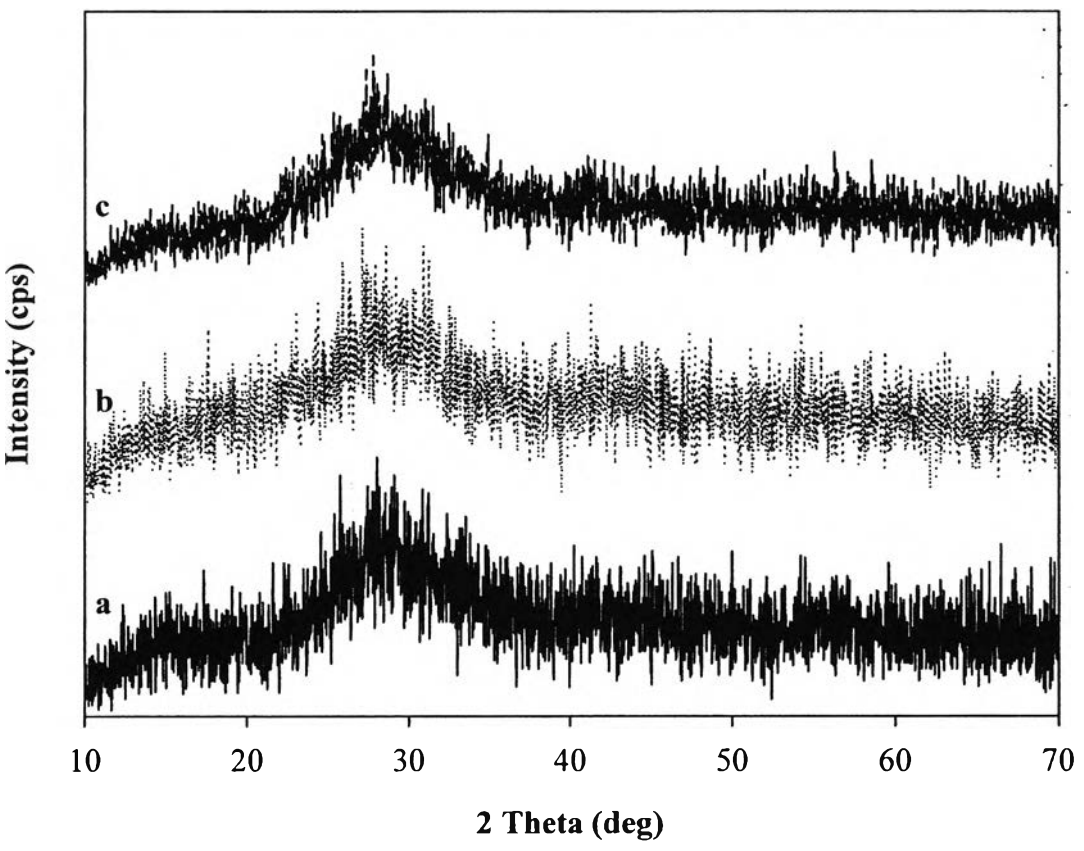

Figure 4.23 XRD patterns of (a) fresh 20%K/mordenite (b) spent catalyst with optimum condition, and (c) treated catalyst.

The BET surface areas of fresh, spent and treated catalysts are demonstrated in Table 4.4. Both K/ZrO_2 and K/mordenite catalysts showed the same trend of result. The spent catalysts had higher surface area than the fresh one because the potassium leaching occurred. After the regeneration, the surface area was increased due to the recovery of active sites after the catalyst was treated by acetone.

For considering the content of potassium on catalysts, the EDS was used and the results are shown in Table 4.4. The potassium content of K/ZrO_2 and K/mordenite catalysts also showed the same tendency. The reduction of potassium content of spent catalysts due to the coverage of oil. This result agrees with the FTIR, SEM, and XRD results. In addition, the potassium content of the treated catalyst was raised because of the washing by acetone. The disapperance of oil agglomeration led to the increasing of active sites, as supported by the XRD results.

Table 4.4 Surface area and potassium content of the fresh, spent, and treated catalysts

Type of catalyst	Surface area (m^2/g)		Percent K (element)	
	K/ZrO_2	K/Mordenite	K/ZrO_2	K/Mordenite
Fresh catalyst	5.17	3.55	10.22	9.23
Spent catalyst	5.98	4.02	7.47	3.75
Treated catalyst	6.30	4.62	8.25	5.23

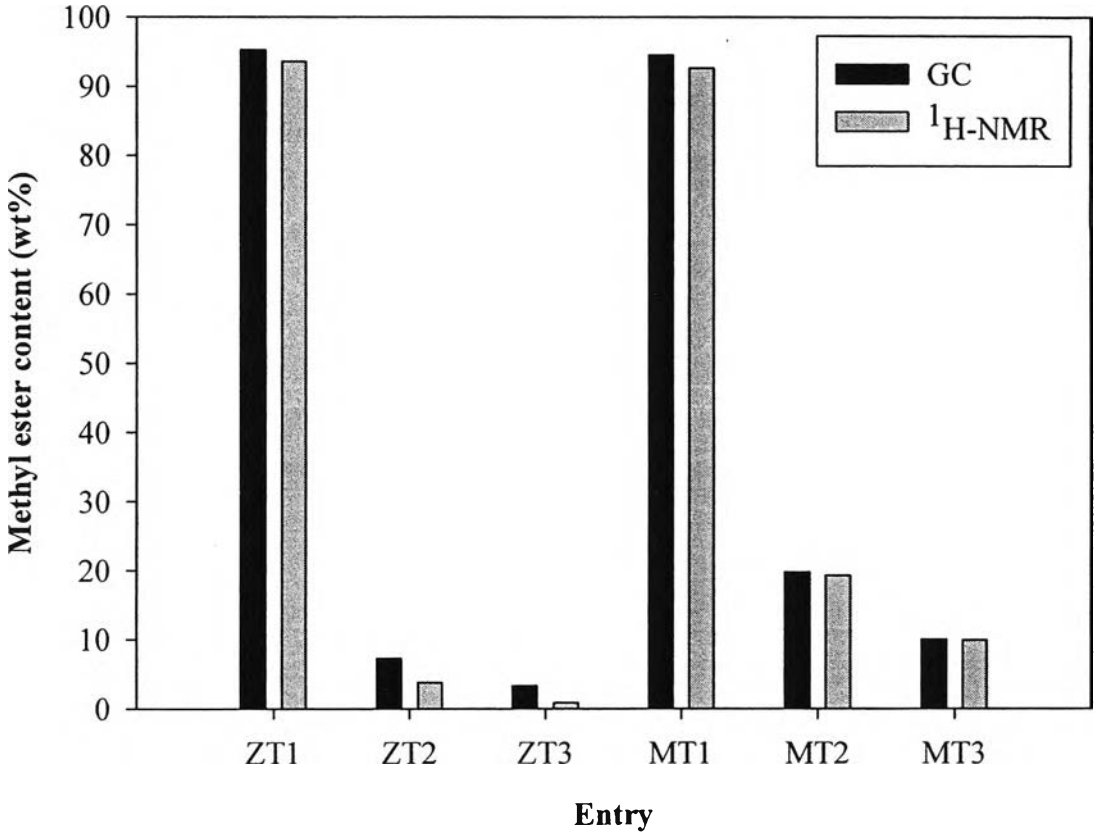

Figure 4.24 Methyl ester content as a function of run numbers of catalyst with pretreatment by acetone. (ZT: K/ZrO_2 with no. of cycle, MC: K/mordenite with no. of cycle) Reaction conditions: a methanol-to-oil molar ratio of 15:1; a reaction temperature of 60°C; a flow rate of 11 ml/min; a catalyst amount 12 wt% with 40–50 mesh; and a reaction time of 6 and 4 hours for KOH/ZrO_2 and KOH/mordenite catalyst, respectively.

4.2.4.2 Biodiesel Analysis

The methyl ester content of three-cycle reaction with catalyst treated with acetone was analyzed by GC and ^{1}H-NMR, as seen in Figure 4.24. From this result, the significant decrease in catalytic activity still occurred. For K/ZrO_2, the conversion of fresh catalysts was declined from 95.29 wt% to 7.28 wt% with the treated catalyst in cycle 2, and only 3.34 wt% with the treated catalyst in cycle 3. Meanwhile, the treated K/mordenite catalyst also gave the reduction of methyl ester

content from 94.54 wt% in cycle 1 with the fresh catalyst to 19.76 wt% in cycle 2 with the treated catalyst, and 10.34 wt% with treated catalyst in the last run. This result was similar to the three-cycle reaction of catalyst without pretreatment, as shown in Figure 4.17. It could be referred that treating with acetone cannot be used to improve the catalytic activity. However, the results from many techniques, such as FTIR, SEM, XRD, BET and EDS, could insist that treating with acetone made the modification of surface catalyst. It could wash the oil, which deposited upon the exterior surface of catalyst and agglomerated on the active sites. Nevertheless, the potassium leaching during reaction could be occurred and only treating with the washing by acetone would not create the number of active sites. Thus, the development of catalytic activity might not be happened.

4.3 Process Phenomenon of Reaction

From the reaction and catalyst characterization, it could be explained the phenomenon of the reaction, as shown in Figure 4.25.

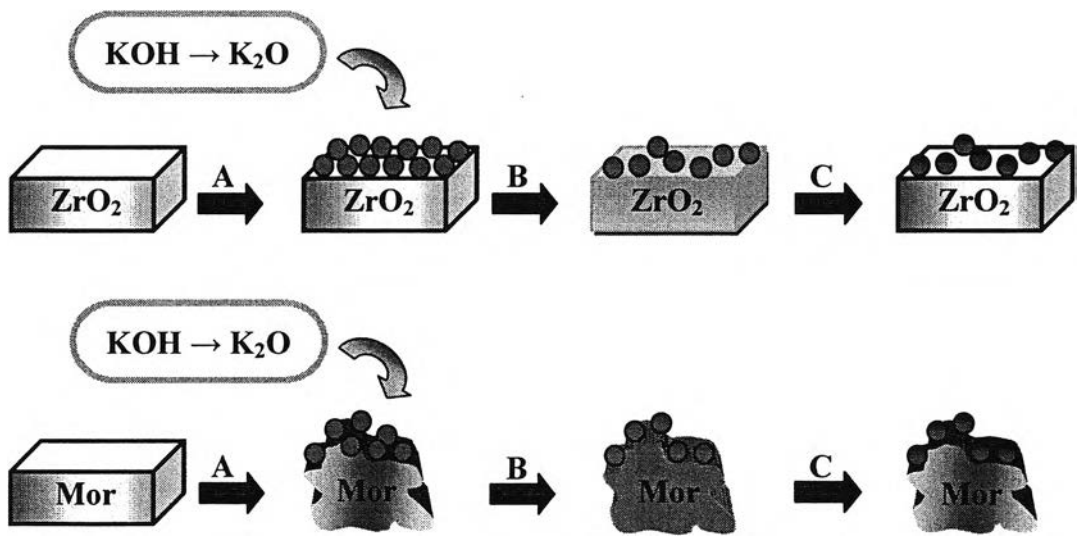

Figure 4.25 The model structure of catalyst phenomenon in transesterification: (●) K_2O, (A) impregnation with 20%K, (B) transesterification reaction, (C) catalyst regeneration, (I) pure support, (II) fresh catalyst, (III) spent catalyst, and (IV) treated catalyst.

Both two types of catalyst, ZrO_2 and mordenite, had the similar phenomenon during the reaction, as shown in Figure 4.25. The pure support was impregnated with 20%K from KOH solution. The decomposition of KOH occurred and it was transformed to K_2O, which was the active sites and attached to the pore of support. For the ZrO_2 support, the loading of K did not change the structure of ZrO_2; however, the modification of mordenite zeolite structure occurred. After the transesterification, some K_2O was leached out from catalyst during reaction. The oil was deposited upon the catalyst surface and agglomerated the remainder of active sites. That would be the cause of the reduction of conversion with the spent catalyst without pretreatment. The catalyst regeneration, by means of acetone flow, cleaned the catalyst surface by washed the oil deposited out. It did not accelerated the activity of catalyst. So, the conversion was not improved.

4.4 Comparison between Biodiesel Production from Batch and Fixed-bed Reactors

The comparison between two different types of reactor for biodiesel production using 20%K/ZrO_2 and 20%K/mordenite as solid catalysts is shown in Table 4.5. This is the comparison between batch experiment (Iangthanarat, 2008) and a fixed-bed reactor in this study. The batch experiment took a shorter reaction time to obtain the higher methyl ester content than a fixed-bed reactor. It could be explained that, in the batch system, the reactant, methanol, and catalyst are stirred and mixed together all the time. That is easily to make the reaction complete. In other way, the fixed-bed system, the reactant and methanol passed through the packed catalyst at a period of time. The contact time of reactant and catalyst was rather short, leading to the longer reaction time. In the point of catalyst size, the optimum catalyst particle size of the batch reactor was 10–20 mesh. However, 40–50 mesh is the optimum catalyst particle size of the fixed-bed reactor. It could be explained that the small particle size was suitable for the fixed-bed reactor because the higher surface area of catalyst increased the higher contact area between reactant and catalyst, leading to high percentage of product.

Table 4.5 Comparison between the batch and fixed-bed reactors for biodiesel production using 20%K/ZrO_2 and 20%K/mordenite as solid catalysts

Reaction parameter	20%K/ZrO_2		20%K/mordenite	
	Batch reactor	Fixed-bed reactor	Batch reactor	Fixed-bed reactor
Reaction time (hours)	2	6	3	4
Catalyst particle size (mesh)	10–20	40–50	10–20	40–50
Methyl ester content (wt%)	99.69	95.29	98.40	94.54